ARTICLE

Cholesterol negatively regulates IL-9–producing CD8+ T cell differentiation and antitumor activity

Xingzhe Ma[1]*, Enguang Bi[1]*, Chunjian Huang[1], Yong Lu[1], Gang Xue[1], Xing Guo[1], Aibo Wang[2], Maojie Yang[1], Jianfei Qian[1], Chen Dong[2], and Qing Yi[1]

CD8+ T cells can be polarized into IL-9–secreting (Tc9) cells. We previously showed that adoptive therapy using tumor-specific Tc9 cells generated stronger antitumor responses in mouse melanoma than classical Tc1 cells. To understand why Tc9 cells exert stronger antitumor responses, we used gene profiling to compare Tc9 and Tc1 cells. Tc9 cells expressed different levels of cholesterol synthesis and efflux genes and possessed significantly lower cholesterol content than Tc1 cells. Unique to Tc9, but not other CD8+ or CD4+ T cell subsets, manipulating cholesterol content in polarizing Tc9 cells significantly affected IL-9 expression and Tc9 differentiation and antitumor response in vivo. Mechanistic studies showed that IL-9 was indispensable for Tc9 cell persistence and antitumor effects, and cholesterol or its derivatives inhibited IL-9 expression by activating liver X receptors (LXRs), leading to LXR Sumoylation and reduced p65 binding to *Il9* promoter. Our study identifies cholesterol as a critical regulator of Tc9 cell differentiation and function.

Introduction

Cancer immunotherapies using adoptive T cell transfer have achieved great success (Rosenberg et al., 2008; Restifo et al., 2012). CD8+ T cells play a central role in antitumor immunity, and many studies have focused on improving the effectiveness of transferred CD8+ T cells, such as priming transferred T cells with different cytokines (Klebanoff et al., 2004, 2005; Hinrichs et al., 2008), transferring tumor-specific CD8+ T cells at various stages of differentiation (Gattinoni et al., 2005, 2011), manipulating signaling pathway and transcription factors (Gattinoni et al., 2009; Miyagawa et al., 2012), and using immune checkpoint blockade (Topalian et al., 2015) or combined treatment (Twyman-Saint Victor et al., 2015; Yang et al., 2016).

Similar to helper CD4+ T cell subsets, CD8+ T cells are capable of differentiating into Tc1, Tc2, Tc9, and Tc17 cells under various cytokine conditions, each of which has a unique cytokine secretion and transcription factor expression pattern (Mittrücker et al., 2014). Among the CD8+ T cell subsets, Tc1 cells or CTLs are the best-characterized effector CD8+ T cells that play a crucial role in clearance of intracellular pathogens and tumors, whereas the function of Tc17 cells on tumor growth remains controversial (Garcia-Hernandez et al., 2010; Zhang et al., 2014b). We have previously reported that Tc9 cells, a newly established CD8+ T cell subset, exerted stronger antitumor effects compared with Tc1 cells after adoptive

transfer, and these effects were associated with prolonged persistence and conversion to IFN-γ– and granzyme-B (Gzmb)-secreting cells in vivo (Hinrichs et al., 2009; Visekruna et al., 2013; Lu et al., 2014; Mittrücker et al., 2014). However, it is unclear how Tc9 cells are programmed to possess these properties. Having knowledge would accelerate new strategies to improve the efficacy of CD8+ T cells for clinical trials. The aim of this study was to elucidate the underlying mechanisms. Using gene profiling, we observed that Tc9 cells expressed a significantly different level of genes responsible for cholesterol synthesis and efflux than Tc1 cells. Tc9 cells had significantly lower levels of intracellular cholesterol than Tc1 cells and modulating cholesterol content, via pharmacological manipulation or by regulating cholesterol synthesis or efflux genes, in CD8+ T cells promoted or impaired IL-9 expression and Tc9 differentiation as well as their antitumor responses in vivo. Interestingly, this seemed to be unique to Tc9 cells, because manipulating cholesterol did not significantly affect the differentiation of other CD8+ or CD4+ T cell subsets, including Th9 cells, in vitro. Our mechanistic studies showed that IL-9 was critical for Tc9 cell persistence and antitumor function in vivo, and cholesterol or its derivative oxysterols regulated IL-9 expression through liver X receptor (LXR) Sumoylation–NF-κB signaling pathways in the cells.

[1]Department of Cancer Biology, Lerner Research Institute, Cleveland Clinic, Cleveland, OH; [2]Institute for Immunology and School of Medicine, Tsinghua University, Beijing, China.

*X. Ma and E. Bi contributed equally to this paper; Correspondence to Qing Yi: yiq@ccf.org.

Results

Tc9 cell differentiation is associated with a low cholesterol reprogramming profile

Our previous study showed that tumor-specific Tc9 cells displayed greater antitumor effects than Tc1 cells after adoptive transfer (Lu et al., 2014). To elucidate the underlying mechanisms, we performed microarray analyses of in vitro polarized mouse Tc9 and Tc1 cells for 24 h and analyzed the data with Ingenuity Pathway Analysis (IPA). The top increased canonical pathways in Tc9 cells included CD28, ICOS-ICOSL, TGF-β, and IL-9 signaling, which was consistent with the known Tc9 (Th9) phenotype (Kaplan, 2013; Lu et al., 2014). Importantly, we found that PPARα/RXRα signaling, which has multiple functions, including lipid, glucose, and fatty acid metabolism, etc., was significantly decreased in Tc9 cells (Fig. 1 A). IPA analysis of PPARα/RXRα downstream signaling revealed that one striking feature associated with Tc9 cells was the distinct patterns of cholesterol-associated gene expression, i.e., low cholesterol synthesis and high efflux gene expression profiles compared with Tc1 cells (Fig. 1, B and C). To confirm the microarray results, we examined by quantitative RT-PCR (qRT-PCR) the expression of some key genes responsible for cholesterol synthesis, efflux, and transport. First, the expression of 3-hydroxy-3-methylglutaryl-CoA reductase (*Hmgcr*), a rate-limiting enzyme in cholesterol synthesis within the mevalonate pathway (Sharpe et al., 2014), was significantly lower in Tc9 cells than in Tc1 cells (Fig. 1 D). Consistently, the expression of squalene epoxidase (*Sqle*), which is downstream of Hmgcr, was down-regulated in Tc9 cells as compared with Tc1 cells. The expression of *Srebf2*, which preferentially activates genes involved in cholesterol biosynthesis and uptake (Horton et al., 2002; Maxwell et al., 2003), was not changed (Fig. 1 D). Second, Tc9 cells displayed increased expression of cholesterol efflux genes *Abca1* and *Abcg1*, without significant changes in the transport genes *Idol* and *Ldlr*, suggesting that Tc9 cells had active cholesterol export (Fig. 1, E and F). To determine whether the changes in gene expression were associated with cellular cholesterol level, Filipin III staining was used to directly determine the relative cholesterol level by confocal microscopy (Fig. 1, G and H) and flow cytometry (Fig. 1 I), and cholesterol content in Tc1 and Tc9 cells was determined by oxidation-based quantification (Fig. 1 J). As expected, Tc9 cells had significantly lower cellular cholesterol content than Tc1 cells, suggesting that low cholesterol content probably favors Tc9 differentiation.

Cholesterol negatively regulates Tc9 cell differentiation and IL-9 expression

To determine whether cholesterol plays a negative role in Tc9 cell differentiation, we manipulated cholesterol content during Tc9 differentiation by adding cholesterol to the cell culture or by using β-cyclodextrin (β-CD), which is widely used in studies (Christian et al., 1997; Yang et al., 2016) to reduce cellular cholesterol content. The effects of manipulating cholesterol were determined by flow cytometry for Filipin III (Fig. S1 A), a cholesterol oxidation–based method (Fig. S1 B), and confocal microscopy (Fig. S1 C). Microarray analysis showed that manipulating cholesterol content induced a remarkable change in *Il9* expression, but not other cytokines, in differentiating Tc9

cells (Fig. 2 A and Fig. S1 D). IL-9 was significantly up-regulated by β-CD treatment, but was suppressed by addition of cholesterol, suggesting that cholesterol has a specific and negative effect on IL-9 expression in differentiating Tc9 cells. Consistently, qRT-PCR showed that *Il9* mRNA expression was remarkably (50,000-fold, based on expression in Tc1 cells being 1) up-regulated in Tc9 cells upon β-CD treatment (Fig. 2, B and C). β-CD treatment slightly up-regulated *Il9* gene expression in Tc1 cells (20-fold; Fig. S2 A), in other CD8+ T cell subsets (40-fold; Fig. 2 C), and in CD4+ T cell subsets (two- to threefold; Fig. S2 B). In contrast, addition of cholesterol significantly inhibited *Il9* expression in Tc9 cells, but had minor effects on other T cell subsets (Fig. 2, B and C). Furthermore, we examined the effects of manipulating cholesterol on IFNγ production in Th1 or Tc1 cells, IL-9 production in Th9 cells, and IL-17 production in Th17 or Tc17 cells. Results showed that cholesterol manipulation had minor or no effects on Th1, Tc1, Th17, and Tc17 cell differentiation or the cytokine production (Fig. S2, B–D). Manipulating cholesterol affected, to certain extent, IL-9 production in Th9 cells, but had much greater effect on Tc9 cells (Fig. S2, B and E). These findings suggested that manipulating cholesterol content significantly affects the differentiation of Tc9 cells, but only has a minor effect on Th9 or other CD4+ or CD8+ T cell subsets.

We performed a series of experiments to confirm the impact of manipulating cholesterol on Tc9 cells. Results showed that β-CD up-regulated whereas cholesterol down-regulated *Il9* gene expression in Tc9 cells in a dose-dependent manner (Fig. 2 D and Fig. S2 F). Flow cytometry (Fig. 2, E and F) and ELISA (Fig. 2 G) confirmed these results. To determine the translational potential of these findings, we examined the impact of manipulating cholesterol on human Tc9 cells. Consistent with mouse results, β-CD up-regulated, whereas cholesterol down-regulated, *Il9* gene expression (Fig. S2 G) and IL-9 production in human Tc9 cells (Fig. 2, H and I). Because CD8+ T cells have the capacity for secondary expansion after a reencounter with antigen (Janssen et al., 2005), we tested IL-9 production in Tc9 cells at 24 and 48 h after restimulation. The IL-9 level remained high in β-CD–treated Tc9 (β-CD-Tc9) cells, but was low in cholesterol-treated Tc9 (Cho-Tc9) cells (Fig. 2 J). Moreover, after 5 d of polarization in the presence of cholesterol or β-CD, Cho-Tc9 and β-CD-Tc9 cells were washed and then cultured in normal T cell culture medium for another 5 d; still, these β-CD-Tc9 cells maintained high *Il9* expression, whereas Cho-Tc9 cells had low *Il9* expression (Fig. S2 H). Furthermore, simvastatin and lovastatin, two inhibitors of Hmgcr that are available as generic products for reducing plasma cholesterol (Tobert, 2003), were used to determine whether inhibiting endogenous cholesterol biosynthesis could also up-regulate IL-9 expression in Tc9 cells. Similar to β-CD treatment, both simvastatin and lovastatin up-regulated IL-9 expression and production in Tc9 cells (Fig. 2, K and L; and Fig. S2, I–K). Furthermore, we used shRNAs to knockdown cholesterol synthesis gene *Hmgcr* and efflux gene *Abca1* (Fig. S3 A), which were the most significantly changed genes in Tc9 cells (Fig. 1, C and D). *Hmgcr* gene knockdown efficiently decreased cholesterol content (Fig. S3 B) and dramatically increased IL-9 expression (Fig. 2 M) and production (Fig. 2 N) in Tc9 cells. Addition of cholesterol reversed the effect of *Hmgcr* knockdown
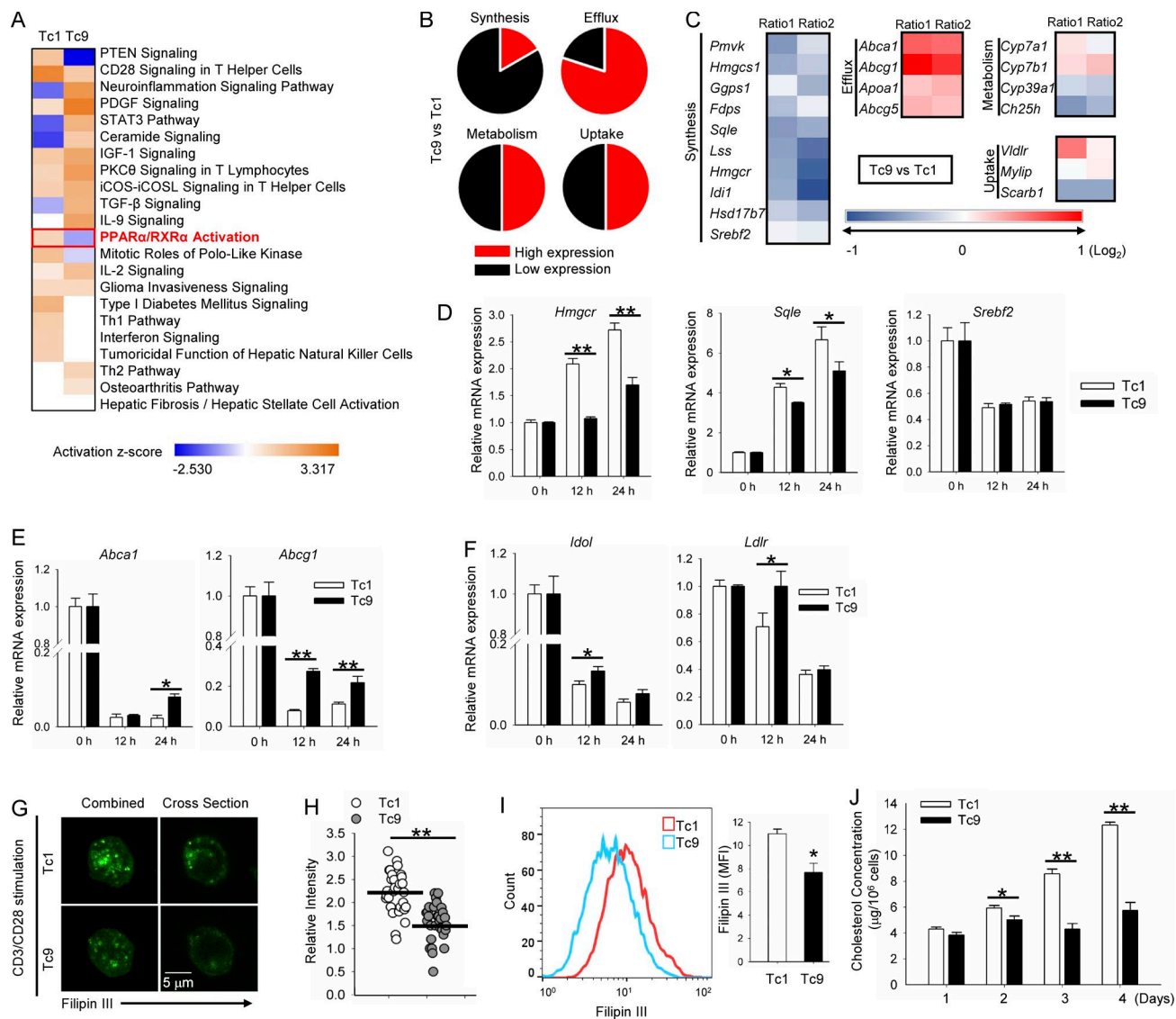
Figure 1. **Tc9 cells display low cholesterol synthesis and high cholesterol efflux gene expression patterns and low cholesterol content compared with Tc1 cells.** CD8+ T cells were in vitro stimulated and differentiated with CD3/CD28 antibodies in the presence of corresponding polarizing cytokines. **(A)** IPA analysis of canonical signaling pathways in Tc9 versus Tc1 cells, 24 h after in vitro differentiation. **(B and C)** Microarray analysis of cholesterol-related gene expression in Tc9 versus Tc1 cells, 24 h after in vitro differentiation. Results represent percentage of total gene changes in each indicated group (B) and relative expression of representative genes (C). Microarray analysis represents two independent experiments. **(D–F)** qRT-PCR analysis of the expression of cholesterol synthesis genes *Hmgcr*, *Sqle*, and *Srebf2* (D), efflux genes *Abca1* and *Abcg1* (E), and transport genes *Idol* and *Ldlr* (F) in Tc9 versus Tc1 cells at indicated time points. **(G–I)** Relative cholesterol content in Tc9 versus Tc1 cells determined by Filipin III staining at day 3 after in vitro differentiation, using confocal microscopy (G), relative quantification of confocal data (H), and flow cytometry (I). MFI, mean fluorescence intensity. **(J)** Cholesterol quantification of Tc9 versus Tc1 cells using a cholesterol oxidation–based method at indicated days after stimulation and differentiation. Experiments were performed with at least three biological replicates and are representative of at least three independent experiments. Data are presented as mean ± SEM. *, $P < 0.05$; **, $P < 0.01$.

(Fig. 2, M and N). On the contrary, cholesterol content was significantly increased (Fig. S3 B) while IL-9 expression (Fig. 2 O) and production (Fig. 2 P) were decreased in *Abca1*-knockdown Tc9 cells. Removal of cholesterol reversed the effect of *Abca1* knockdown (Fig. 2, O and P).

To reconfirm that high cholesterol repressed Tc9 differentiation, *Apoe*−/− mice, an atherosclerosis-prone transgenic mouse with high plasma and cellular cholesterol levels (Zhang et al., 2014a) were used. IL-9 expression and production were both impaired in Tc9 cells from *Apoe*−/− as compared with WT mice (Fig. S3 C). Collectively, these data clearly demonstrated

that cholesterol is detrimental to Tc9 cell differentiation and IL-9 expression.

Reducing cholesterol enhances Tc9 cell persistence and antitumor activity in an IL-9–dependent manner in vivo

Compared with Tc1 cells, Tc9 cells persist longer in vivo after transfer (Lu et al., 2014). Therefore, we sought to determine whether cholesterol modulation could further improve the persistence and antitumor activity of Tc9 cells. Pmel-1–derived Tc1, Tc9, β-CD-Tc9, or Cho-Tc9 cells were transferred into MC38-gp100 tumor–bearing C57BL/6 mice (Fig. S4 A). We collected blood at
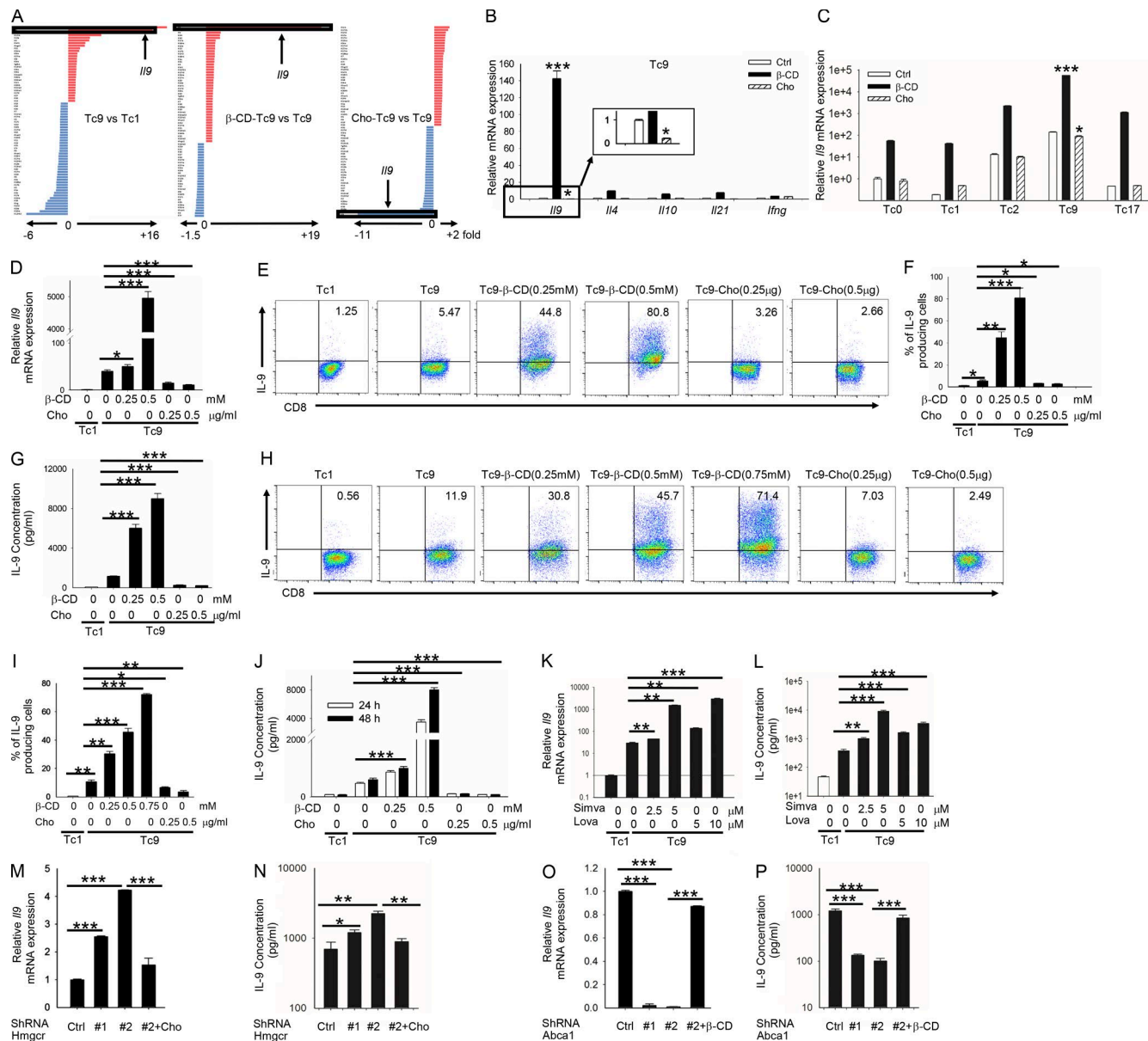
Figure 2. **Cholesterol negatively regulates while reducing cholesterol enhances Tc9 cell differentiation.** CD8^{+} T cells were in vitro stimulated and differentiated with CD3/CD28 antibodies under corresponding polarizing conditions, with indicated treatments during the entire process. **(A)** Microarray analysis of Tc1, Tc9, β-CD-Tc9, and Cho-Tc9 cell cytokine and cytokine receptor expression at day 5 after in vitro differentiation. **(B)** qRT-PCR analysis of *Il9*, *Il4*, *Il10*, *Il21*, and *Ifng* expression in Tc9, β-CD-Tc9, and Cho-Tc9 cells at day 5 after in vitro differentiation. **(C)** qRT-PCR analysis of *Il9* expression in Tc0, Tc1, Tc2, Tc9, and Tc17 cells with or without β-CD or Cho treatment at day 5 after in vitro differentiation. **(D)** Transcriptional levels of *Il9* in Tc1, Tc9, β-CD-Tc9, and Cho-Tc9 cells at day 5 after in vitro differentiation. **(E and F)** Flow cytometry analysis of IL-9–producing cells in Tc1, Tc9, β-CD-Tc9, and Cho-Tc9 cells at day 4 after in vitro differentiation. **(G)** ELISA quantification of IL-9 production in supernatants of Tc1, Tc9, β-CD-Tc9, and Cho-Tc9 cells at day 4 after in vitro differentiation. **(H and I)** Flow cytometry analysis of IL-9–producing cells in Tc1, Tc9, β-CD-Tc9, and Cho-Tc9 cells differentiated from human blood CD8^{+} T cells at day 4 after in vitro differentiation. β-CD or cholesterol was present during the entire culture process. **(J)** In vitro differentiated Tc1 and Tc9 cells with indicated treatments were counted, and the same number of cells were taken and restimulated at day 5 for another 1 or 2 d. Supernatants were collected and examined for IL-9 production by ELISA. **(K and L)** Transcriptional levels of *Il9* expression (K) and ELISA quantification of IL-9 production (L) in Tc1, Tc9, simvastatin-treated Tc9, and lovastatin-treated Tc9 cells at day 4 after in vitro differentiation. Simva, simvastatin; Lova, lovastatin. **(M and N)** Transcriptional levels of *Il9* expression (M) and ELISA quantification of IL-9 production (N) in Tc9 (Ctrl), *Hmgcr*-knockdown (shRNA #1 and #2, two different shRNAs) Tc9, and cholesterol-treated *Hmgcr*-knockdown (#2 + Cho) Tc9 cells at day 5 after in vitro differentiation. **(O and P)** Transcriptional levels of *Il9* expression (O) and ELISA quantification of IL-9 production (P) in Tc9 (Ctrl), *Abca1*-knockdown (shRNA #1 and #2, two different shRNAs) Tc9, and β-CD–treated *Abca1*-knockdown (#2 + β-CD) Tc9 cells at day 5 after in vitro differentiation. Experiments were performed with at least three biological replicates and are representative of at least two independent experiments. β-CD, β-cyclodextrin–treated; Cho, cholesterol-treated. Data are presented as mean ± SEM. *, P < 0.05; **, P < 0.01; ***, P < 0.001.

various time points and examined the percentage and number of transferred Tc9 or Tc1 cells. The number of Tc9 cells was significantly greater than the number of Tc1 cells at each time point

(Fig. 3 A), confirming that Tc9 cells persisted better in vivo versus Tc1 cells. Compared with Tc9 cells, β-CD–treated Tc9 cells persisted even longer, whereas cholesterol-treated Tc9 cells had poor
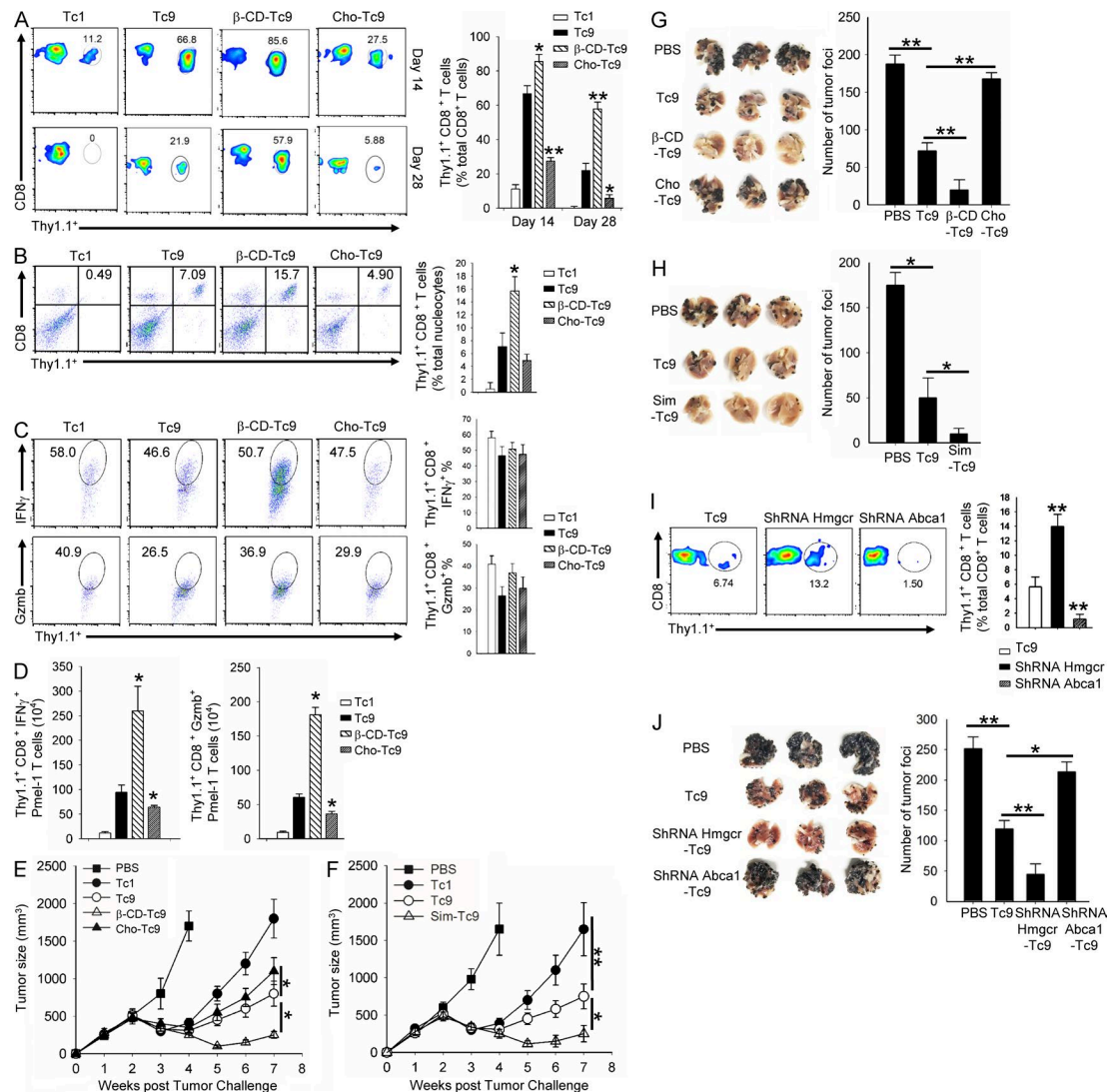
Figure 3. **Reducing cholesterol enhances Tc9 cell persistence and potentiates its antitumor activity in vivo. (A–E)** Pmel-1–derived Tc1, Tc9, β-CD-Tc9, and Cho-Tc9 cells were in vitro differentiated for 5 d and then transferred into MC38-gp100 tumor–bearing mice. Persistence of the transferred T cells was assessed by collecting tail vein blood at 14 and 28 d after transfer using FACS analysis (A). At day 28, tumors in each group were resected, the percentage of tumor-infiltrating transferred total (B) or IFN-γ– and GzmB-producing T cells (C), and the number of tumor-infiltrating transferred IFN-γ– and GzmB-producing cells (D; cell number was normalized to 100 mg tumor tissue) were detected by FACS. Tumor size was measured with calipers and calculated (E). **(F)** Pmel-1–derived Tc1, Tc9, and Sim-Tc9 cells were transferred into MC38-gp100 tumor–bearing mice. Tumor size was measured with calipers. **(G)** Pmel-1–derived Tc9, β-CD-Tc9, and Cho-Tc9 cells were transferred into B16 tumor–bearing mice. After 16 d, mice were sacrificed to enumerate the tumor foci in the lung. **(H)** Pmel-1–derived Tc9 or Sim-Tc9 cells were transferred into B16 tumor–bearing mice. After 16 d, tumor foci in the lung were counted. **(I)** Pmel-1–derived Tc9, *Hmgcr*-knockdown (shRNA Hmgcr) Tc9, and *Abca1*-knockdown (shRNA Abca1) Tc9 cells were transferred into lung B16 tumor-bearing mice. After 7 d, blood was collected to analyze the percentage of transferred cells. **(J)** Pmel-1–derived Tc9, *Hmgcr*-knockdown (shRNA Hmgcr) Tc9, and *Abca1*-knockdown (shRNA Abca1) Tc9 cells were transferred into lung B16 tumor–bearing mice. After 16 d, mice were sacrificed to enumerate the tumor foci in the lung. T cell persistence and tumor growth experiments were performed with five mice per group and are representative of at least two independent experiments. Data are presented as mean ± SEM. *, P < 0.05; **, P < 0.01.

survival (Fig. 3 A). At the end of the fourth week after transfer, significantly higher numbers of β-CD-Tc9 cells, compared with Tc9 or Tc1 cells, were also detected in tumors (Fig. 3 B).

Because Tc9 cells convert to IFN-γ– and GzmB-producing cells in vivo (Lu et al., 2014), we examined whether cholesterol modulation could also have an impact on the percentage and total number of IFN-γ– and GzmB-producing Tc9 cells. Although cholesterol modulation did not affect the percentages of IFN-γ– and GzmB-producing Tc9 cells in vivo (Fig. 3 C), a significantly higher number of IFN-γ– and GzmB-producing Tc9 cells was detected in

tumors of mice injected with β-CD-Tc9 cells than those injected with Tc9 or Cho-Tc9 cells (Fig. 3 D). Significantly lower numbers of IFN-γ– and GzmB-producing Tc9 cells were detected in tumors from mice injected with Cho-Tc9 cells than those injected with Tc9 cells (Fig. 3 D). At 4 wk after adoptive transfer, among tumor-infiltrating Tc9 and Tc1 cells, cholesterol content remained the lowest in β-CD-Tc9 cells (Fig. S4 B), and β-CD-Tc9 cells maintained high *Il9* expression (Fig. S4 C). To determine why the number of the T cells differed in vivo among Tc9, β-CD-Tc9, and Cho-Tc9, we examined the status of T cell proliferation and apoptosis. No

significant difference was observed in Tc9 proliferation; however, β-CD-Tc9 cells displayed decreased apoptosis, and Cho-Tc9 cells displayed increased apoptosis as compared with control Tc9 cells (Fig. S4, D and E), suggesting that Cho-Tc9 cells had poor survival versus control Tc9 and β-CD-Tc9 cells in vivo. Finally, we determined the antitumor activity of these cells. β-CD-Tc9 cells displayed the best antitumor activity among all groups (Fig. 3 E). We also evaluated simvastatin-treated Tc9 cells (Sim-Tc9) and found that Sim-Tc9 cells, similar to β-CD-Tc9 cells, also had antitumor activity superior to that of Tc9 cells (Fig. 3 F). To confirm the results, we repeated the experiments in a metastatic lung tumor model (Fig. S4 F). Again, β-CD-Tc9 (Fig. 3 G) and Sim-Tc9 (Fig. 3 H) cells displayed the best antitumor activity among Tc9 cells, and Cho-Tc9 cells exerted weaker antitumor activity in vivo than Tc9 cells (Fig. 3, E and G).

To confirm the results, *Hmgcr* and *Abca1* knockdown Tc9 cells were used in vivo. The results showed that *Hmgcr*-knockdown Tc9 cells had significantly longer persistence and better antitumor activity than Tc9 cells in tumor-bearing mice, whereas the in vivo persistence and antitumor function of *Abca1*-knockdown Tc9 cells were drastically impaired in comparison with Tc9 cells (Fig. 3, I and J).

Because a high level of cholesterol is harmful to Tc9 differentiation in vitro and its antitumor activity in vivo, it is interesting to determine whether β-CD-Tc9 cells could function well in host with high levels of cholesterol. We transferred β-CD-Tc9 cells into tumor bearing WT or *Apoe^{-/-}* mice and examined their persistence and antitumor effects. Deficiency of *Apoe* slightly accelerated tumor growth in the host without T cell transfer. β-CD-Tc9 cells displayed slightly impaired persistence, but still exerted a strong antitumor activity in *Apoe^{-/-}*, as compared with WT mice (Fig. S4, G and H). These results suggest that host cholesterol does not significantly impair the function of the T cells.

IL-9 is indispensable for Tc9 cell survival and persistence in vivo

Because persistence and antitumor function seemed to positively correlate to IL-9 production in Tc9 cells, we hypothesized that IL-9 was indispensable for Tc9 persistence and antitumor activity in vivo. To test this hypothesis, we used Pmel-1-WT and Pmel-1-*Il9^{-/-}*-mice (bearing MC38-gp100 tumor) that received adoptive transfer of Pmel-1-WT-Tc9, Pmel-1-*Il9^{-/-}*-Tc9, Pmel-1-*Il9^{-/-}*-β-CD-Tc9, or Pmel-1-*Il9^{-/-}*-Cho-Tc9 cells. Tc9 cells derived from *Il9^{-/-}*-mice do not express *Il9*, but express high levels of the *Il9* transcription factors *Irf4* and *Pu.1* (Fig. S4 I). Compared with WT-Tc9 cells, significantly lower numbers of *Il9^{-/-}*-Tc9 cells were detected in the blood of WT mice, and the numbers of these cells in *Il9^{-/-}* mice were even lower (Fig. 4, A and B). No significant difference was found in the numbers of Tc9, β-CD-Tc9, or Cho-Tc9 cells derived from *Il9^{-/-}* mice. Similar results were obtained from tumor-infiltrating–transferred Tc9 cells (Fig. 4 C). These findings suggested that the prolonged survival of Tc9 cells in vivo depends on Tc9- and host-derived IL-9, and modulating cholesterol does not affect Tc9 cell function when the T cells secrete no IL-9. Although IL-9 deficiency in Tc9 cells did not affect their conversion to IFN-γ– and GzmB-producing cells in vivo (Fig. 4 D), the total number of tumor-infiltrating Thy1.1⁺CD8⁺ IFN-γ– and

GzmB-producing *Il9^{-/-}*-Tc9 cells was significantly lower than WT-Tc9 cells (Fig. 4 E). Indeed, although these T cells showed similar proliferative capacity, *Il9^{-/-}*-Tc9 cells displayed increased apoptosis compared with WT-Tc9 cells (Fig. S4, J and K), indicating poor survival of *Il9^{-/-}*-Tc9 cells in vivo. Thus, these results clearly showed that IL-9 plays a vital role for Tc9 cell survival and persistence in vivo.

To reconfirm that IL-9 secretion helps Tc9 cells to persist longer in vivo, we used the CRISPR/Cas9 technology to knock in a GFP complete coding sequence at the C terminal of IL-9 mRNA by providing a GFP template plasmid as described in Fig. S4, L and M. The percentage of GFP⁺ CD8⁺ T cells was much higher in β-CD Tc9 cells as compared with control Tc9 cells in vitro (Fig. S4 N). Furthermore, we sorted out the GFP⁺ CD8⁺ T cells from control and β-CD Tc9 cells and transferred them into tumor-bearing mice. Similarly, the percentages of GFP⁺ donor CD8⁺ T cells and mean fluorescent intensity of total donor CD8⁺ T cells were much higher in β-CD Tc9 cells as compared with control Tc9 cells at both day 5 and day 12 after transfer (Fig. S4, O and P). Thus, these results prove that IL-9 secretion does help Tc9 cells to persist longer in vivo.

Consistent with poor persistence, *Il9^{-/-}*-Tc9 cells also displayed a compromised antitumor effect compared with WT-Tc9 cells in both subcutaneous MC38-gp100 (Fig. 4 F) and B16 lung metastatic (Fig. 4 G) mouse models, indicating that IL-9 is required for Tc9-mediated antitumor effects in vivo. To confirm these results, Tc9 cells from *Il9r^{-/-}* mice were used. *Il9r^{-/-}*-Tc9 cells did not express *Il9r* (Fig. S4 Q), but secreted large amounts of IL-9 (Fig. S4 R), indicating that IL-9 signaling in the T cells was deficient. As expected, *Il9r^{-/-}*-Tc9 cells also had compromised antitumor activity, and reducing cholesterol in these cells had no effect on their antitumor response in vivo (Fig. 4 H). Collectively, these results indicated that IL-9 and IL-9 signaling in Tc9 cells are indispensable for Tc9 cell persistence and antitumor activity in vivo and that cholesterol modulates the differentiation and function of Tc9 cells by regulating the expression of IL-9.

Cholesterol-derived oxysterols inhibit IL-9 expression via LXR Sumoylation

Next, we elucidated the mechanisms underlying cholesterol-mediated regulation of IL-9 expression in Tc9 cells. First, we examined whether modulation of cholesterol affected TCR signaling in the cells, because cholesterol is important for regulating TCR signaling (Swamy et al., 2016; Yang et al., 2016). However, no significant differences in TCR signaling were found in Tc9, β-CD-Tc9, or Cho-Tc9 cells (Fig. S5 A). Second, because cholesterol manipulation by β-CD, lovastatin, or simvastatin did not affect the expression of the *Il9* transcription factors Irf4 and Pu.1 (Fig. S5 B), we ruled out the involvement of these transcriptional factors. To understand how cholesterol regulates IL-9 expression in the cells, we again used IPA analysis to examine the gene microarray data obtained from CD8⁺ T cells with and without cholesterol treatment. Interestingly, we found that only LXR/RXR signaling was activated (Fig. 5 A) in the T cells after cholesterol treatment, suggesting that cholesterol-induced inhibitory effect may be mediated by the LXR/RXR signaling. Because cholesterol derivatives participate in various signaling pathways (Traversari et al., 2014),
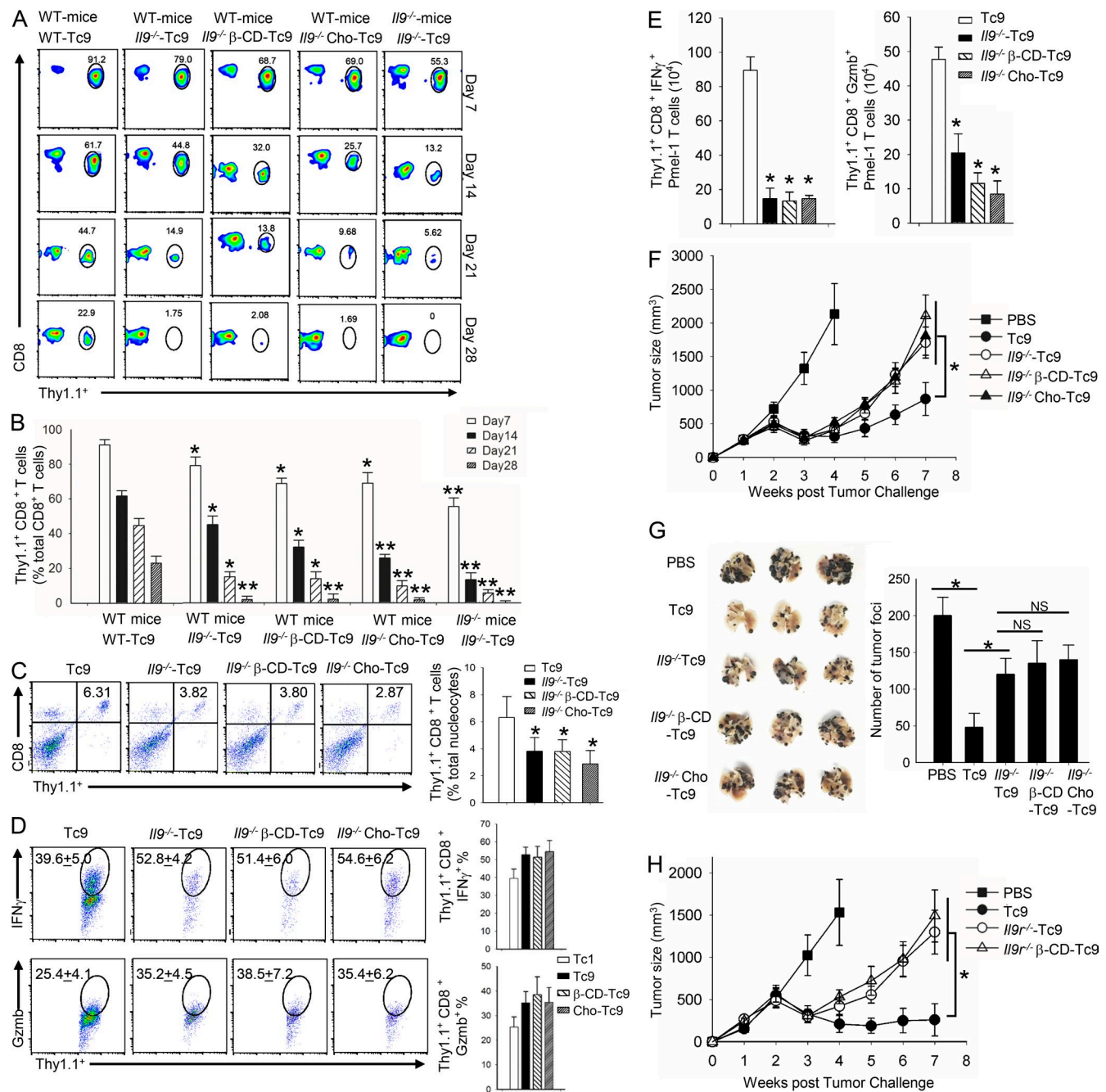
Ma et al.
Cholesterol negatively regulates Tc9 cells

Journal of Experimental Medicine
https://doi.org/10.1084/jem.20171576

1560

Figure 4. IL-9 is indispensable for Tc9 cell survival and persistence in vivo. (A–F) Tc9, β-CD-Tc9, and Cho-Tc9 cells from Pmel-1 WT or Pmel-1-*Il9⁻/⁻* mice were transferred into MC38-gp100 tumor–bearing WT or *Il9⁻/⁻* mice as indicated. Persistence of the cells was determined using FACS analysis by collecting tail vein blood for consecutive 4 wk after transfer (A and B). In B, statistical comparison was always made with control Tc9 cells. **(C–E)** At day 28, tumors in each group were resected and the percentage of tumor-infiltrating transferred total (C) or IFN-γ– and GzmB-producing T cells (D) and the number of tumor-infiltrating transferred IFN-γ– and GzmB-producing cells (E; cell number was normalized to 100 mg tumor tissue) were detected by FACS. Tumor size was measured with calipers and calculated (F). **(G)** Tc9 cells from Pmel-1 WT mice and Tc9, β-CD-Tc9, or Cho-Tc9 cells from Pmel-1-*Il9⁻/⁻* mice were transferred into B16 tumor–bearing mice. After 16 d, tumor foci in the lung were counted. **(H)** Tc9 or β-CD-Tc9 cells from Pmel-1 WT or Pmel-1-*Il9r⁻/⁻* mice were transferred into MC38-gp100 tumor–bearing mice. Tumor size was measured with calipers and calculated. T cell persistence and tumor growth experiments were performed with five mice per group and are representative of at least two independent experiments. Data are presented as mean ± SEM. *, P < 0.05; **, P < 0.01. NS, not significant.

we differentiated Tc9 cells in the presence of cholesterol, various oxysterols, and sterol-related compounds to determine whether cholesterol derivatives inhibited IL-9 expression. Indeed, cholesterol and all oxysterols, including 22(R)-hydroxycholesterol, but not 22(S)-hydroxycholesterol or other cholesterol derivatives, inhibited *Il9* mRNA expression and IL-9 secretion (Fig. 5, B and C).

22(R)-hydroxycholesterol and 22(S)-hydroxycholesterol are stereoisomers (Joseph et al., 2003). Our results showed that 22(R)-hydroxycholesterol inhibited IL-9 expression and production, but 22(S)-hydroxycholesterol did not (Fig. 5, B and C). The different effects of these two stereoisomers on IL-9 expression led us to focus on their functions. Oxysterols can activate LXRs,
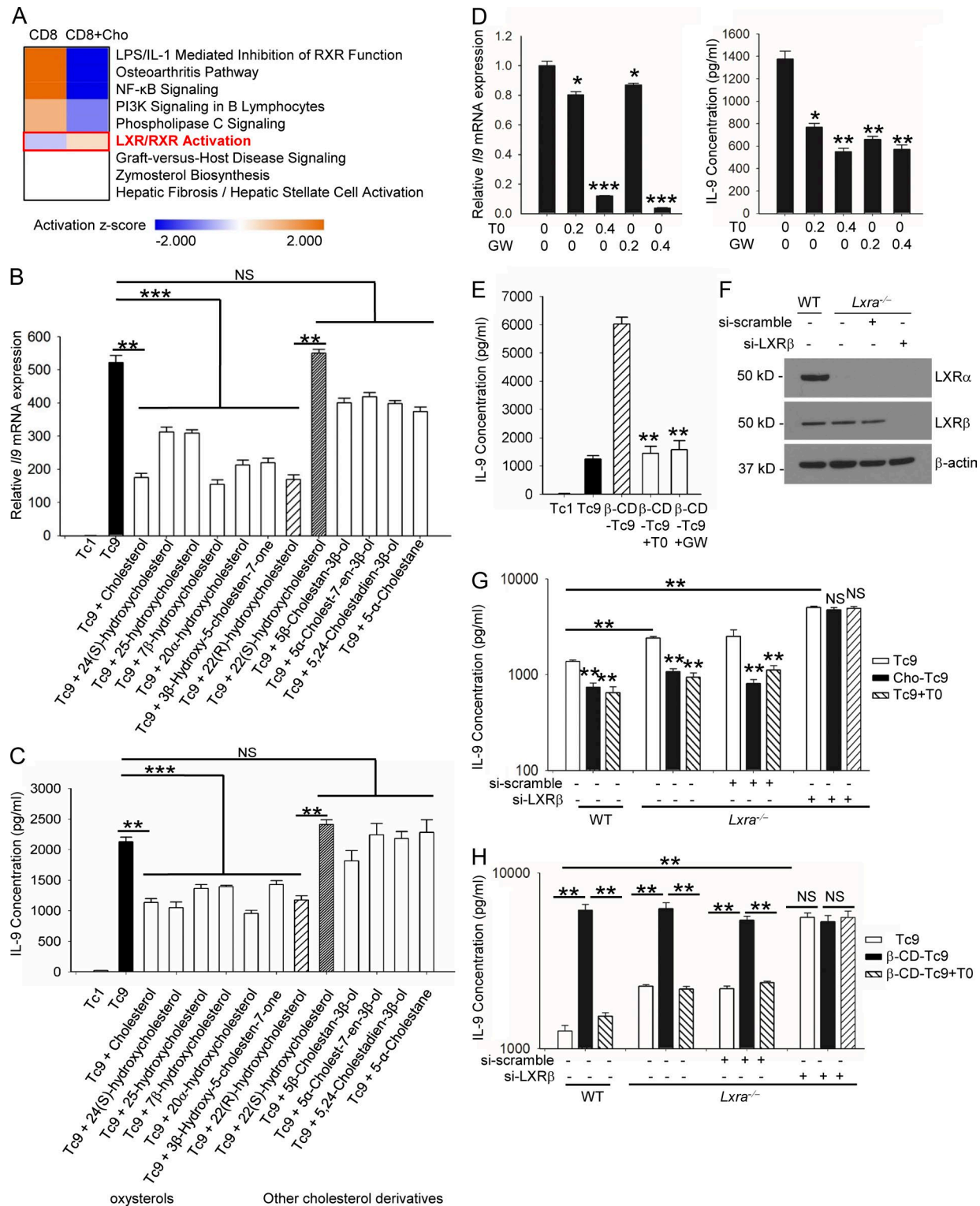
Figure 5. **Oxidized cholesterol–mediated LXR activation inhibits IL-9 expression.** CD8+ T cells were in vitro stimulated and differentiated with CD3/CD28 antibodies under the Tc9-polarizing condition with the indicated treatments during the entire process. **(A)** IPA analysis of canonical signaling pathways in 24 h–cultured CD8+ cells treated, with or without cholesterol. Microarray analysis data represents two independent experiments. **(B and C)** qRT-PCR of *Il9* mRNA expression (B) and ELISA detection of IL-9 production (C) in Tc9 cells at day 4 after in vitro differentiation with indicated treatments. Shaded bars represent IL-9 expression in control Tc9 and Tc9 cells treated with 22(R)- or 22(S)-hydroxycholesterols. **(D)** IL-9 expression (left) and production (right) in Tc9 cells with or without T0 or GW3965 (GW) treatment as indicated at day 4 after in vitro differentiation. **(E)** ELISA detection of IL-9 production in Tc9 cells with or without β-CD and T0 or GW treatment at day 4 after in vitro differentiation. **(F–H)** CD8+ T cells from *Lxra*−/− mice were in vitro stimulated and differentiated with CD3/CD28 antibodies under the Tc9-polarizing condition for 1 d and then transfected with LXRβ siRNA for 1 d, followed by indicated treatments for additional 2 d. *Lxra* knockout and LXRβ knockdown efficiency were examined before treatment (F), and IL-9 production was measured under the indicated conditions (G and H). Experiments were performed with at least three biological replicates and are representative of at least two independent experiments. Data are presented as mean ± SEM. *, P < 0.05; **, P < 0.01; ***, P < 0.001.

which are "cholesterol sensors" (Joseph et al., 2003; Traversari et al., 2014). 22(R)-hydroxycholesterol can act as a LXR ligand, whereas 22(S)-hydroxycholesterol is inactive (Joseph et al., 2003). These data further suggest that LXR signaling mediates the effect of cholesterol on the suppression of IL-9 expression. To confirm whether LXRs were involved in regulating IL-9 expression, we used two synthetic LXR agonists, T0901317 (T0) and GW3965 (Bełtowski, 2008), to activate LXRs in differentiating Tc9 cells. Both T0 and GW3965, similar to the effects of oxysterols, significantly inhibited IL-9 expression and production in Tc9 cells (Fig. 5 D). Moreover, we treated β-CD–Tc9 cells with T0 or GW3965 during differentiation, and both abrogated β-CD–mediated up-regulation of IL-9 expression in Tc9 cells (Fig. 5 E). Together with IPA analysis, these results demonstrated that LXR signaling mediates IL-9 inhibition by cholesterol. To determine whether cholesterol-mediated inhibition of IL-9 expression in Tc9 cells was LXR dependent, we isolated CD8$^+$ T cells from $Lxra^{-/-}$ mice and knocked down their $Lxrb$ gene with siRNA (Fig. 5 F), because both LXRα and LXRβ may be important in regulating IL-9 expression (Joseph et al., 2003). Tc9 cells deficient in LXRs secreted significantly more IL-9 than WT-Tc9 cells (Fig. 5 G). Cholesterol or T0 inhibited IL-9 expression in WT-Tc9, but not in LXR-deficient Tc9 cells (Fig. 5 G). Consistently, although β-CD up-regulated IL-9 expression in Tc9 cells, whereas T0 abrogated such an effect, these agents had no effect on IL-9 production in LXR-deficient Tc9 cells (Fig. 5 H). Thus, these results indicated that cholesterol-mediated inhibition of IL-9 production in Tc9 cells indeed depends on LXRs.

Next we investigated how LXRs regulated IL-9 expression in CD8$^+$ T cells. Because LXR activation repressed $Il9$ transcription (Fig. 5 D), we examined whether cholesterol manipulation with β-CD and T0 treatment could affect LXR expression and its modification by Sumoylation. Although no differences were observed in LXRs and Sumo1, -2, and -3 expression upon β-CD and T0 treatment (Fig. 6 A and Fig. S5 C), β-CD repressed Sumoylation of LXRα (Sumo2 and -3) and LXRβ (Sumo1). T0 treatment abrogated the effects of β-CD on LXR Sumoylation. To determine whether Sumoylation could directly inhibit IL-9 expression, the Sumoylation inhibitor 2-D08 was used. As expected, 2-D08 significantly increased IL-9 expression and production in treated cells (Fig. 6, B and C). To verify whether LXR Sumoylation mediated the inhibition of IL-9 expression, LXRβ-knockdown CD8$^+$ T cells from $Lxra^{-/-}$ mice were used (Fig. S5 D). As expected, 2-D08 was no longer able to up-regulate IL-9 production in these T cells (Fig. 6 D), indicating that LXR Sumoylation inhibits IL-9 production in Tc9 cells.
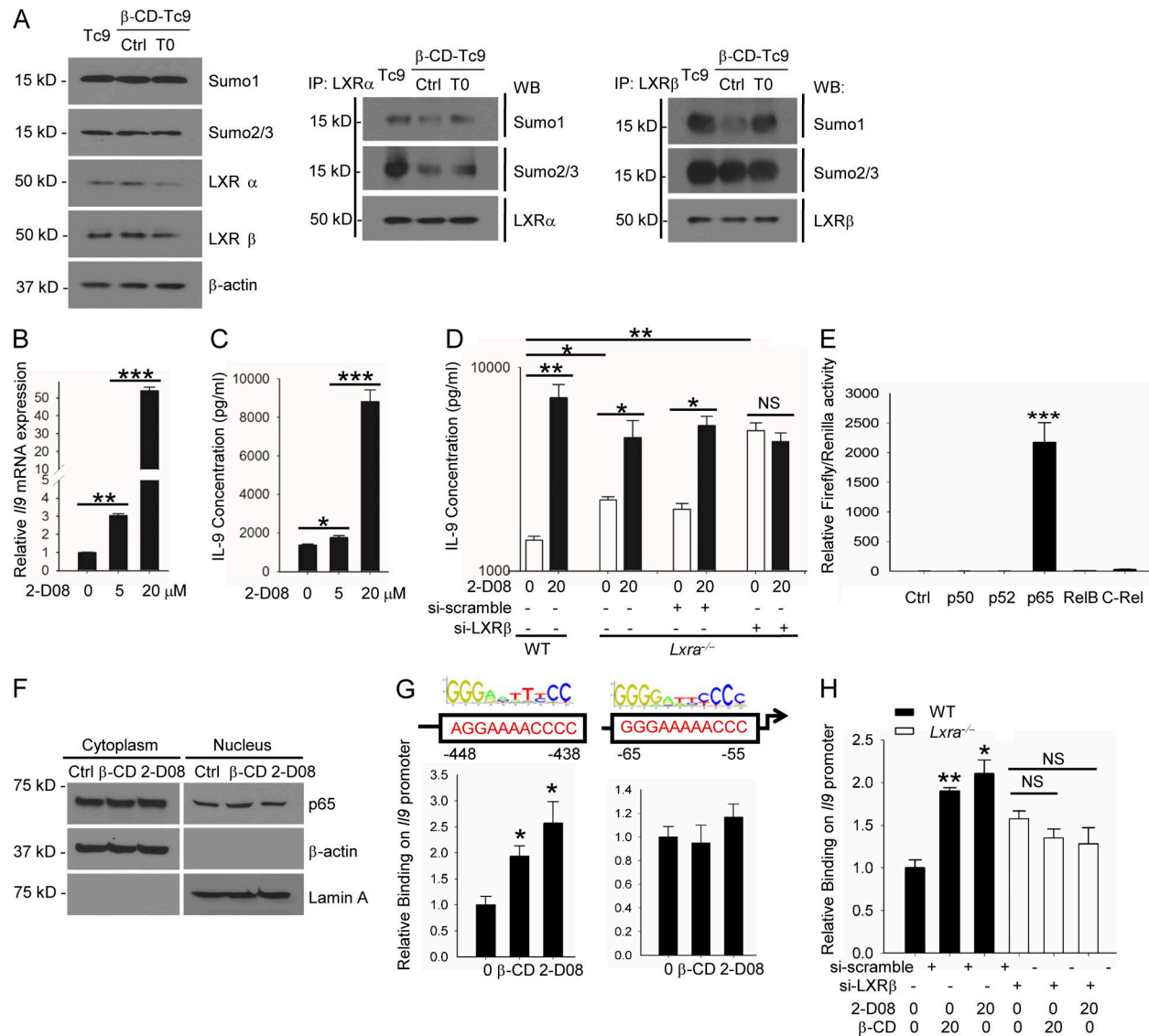
Finally, we attempted to identify transcription factors downstream of cholesterol and LXRs that regulated IL-9. We sought to determine whether NF-κB, which was reported to be important for CD4$^+$ Th9 cell differentiation (Xiao et al., 2012), may also play a role in Tc9 cells. First, a luciferase reporter assay was performed to examine which NF-κB subunits bind and transcribe the $Il9$ gene. As shown in Fig. 6 E, p65, but not other members of the NF-κB complex, strongly activated $Il9$ transcription. Interestingly, inhibition of Sumoylation by either β-CD or 2-D08 did not affect p65 expression or nuclear translocation (Fig. 6 F), but significantly increased the binding of p65 to one of the NF-κB

binding sites on the $Il9$ promoter in Tc9 cells as demonstrated by ChIP assay (Fig. 6 G). To determine whether the enhanced p65 binding was indeed induced by inhibition of LXR Sumoylation, another ChIP assay was performed. As shown in Fig. 6 H, inhibition of Sumoylation by either β-CD or 2-D08 significantly increased p65 binding on the $Il9$ promoter in WT-Tc9, but not in LXR-deficient Tc9 cells. Hence, these data indicated that cholesterol-induced LXR Sumoylation inhibits IL-9 expression, at least in part, by reducing the binding of p65 to $Il9$ promoter in the cells.

Discussion

This study reports an interesting and novel finding that cholesterol or its derivatives play an important role in Tc9 cell differentiation and function in vivo. We showed that Tc9 cells expressed different levels of genes responsible for cholesterol synthesis and efflux, and Tc9 cells had a significantly lower level of cholesterol content than Tc1 cells. Modulating cholesterol content in CD8$^+$ T cells promoted or impaired IL-9 expression and Tc9 cell differentiation as well as their antitumor responses in vivo. These effects were unique to Tc9 cells because manipulating cholesterol had only minor or no effects on other subsets of CD4$^+$ and CD8$^+$ T cells, including Th9 cells. Our results further showed that Tc9 cells deficient in IL-9 or IL-9 receptor had significantly impaired in vivo persistence and antitumor effects as compared with WT-Tc9 cells, indicating the importance of IL-9 and IL-9 signaling for the persistence and antitumor function of Tc9 cells. Furthermore, $Il9^{-/-}$-Tc9 cells transferred into $Il9^{-/-}$ mice displayed worse persistence than cells transferred into WT mice, suggesting that host-derived IL-9 also plays a role in Tc9 cell function. Finally, our mechanistic studies showed that cholesterol or its derivative oxysterols regulated IL-9 expression through LXR Sumoylation and NF-κB signaling pathways.

A lipid anabolic program is required for membrane biosynthesis and cellular growth during T cell activation. Cholesterol modulates the function of membrane proteins, participates in membrane trafficking, and regulates transmembrane signaling. Cholesterol metabolites also act as signal transducers (Ikonen, 2008; Spann and Glass, 2013). Recent studies show that inhibition of cholesterol esterification can enhance T cell receptor clustering and signaling in CD8$^+$ T cells, whereas other studies suggest that cholesterol sulfate represses T cell activation by inhibiting the phosphorylation of intracellular immunoreceptor tyrosine-based activation motifs in TCRs (Wang et al., 2016; Yang et al., 2016). Yang et al. reported that inhibition of cholesterol esterification (which increased free cholesterol content in cells) enhanced the antitumor function of CD8$^+$ T cells, indicated by increased immunological synapse formation, TCR signaling, and enhanced GzmB and IFN-γ secretion. In contrast, in our study, reducing cholesterol content under the Tc9-polarizing condition significantly potentiated the antitumor function of Tc9 cells, which was associated with longer in vivo persistence and higher IL-9 production as compared with control Tc9 or Tc1 cells. This discrepancy in the results may be caused by differences in cholesterol metabolism across specific cytokine differentiation or polarization conditions in CD8$^+$ T cells (Yang et al., 2016). Hu et al. also reported that sterol metabolism could generate endogenous

Ma et al.
Cholesterol negatively regulates Tc9 cells

Journal of Experimental Medicine 1563
https://doi.org/10.1084/jem.20171576

Figure 6. **LXR activation-induced LXR-Sumoylation inhibits IL-9 expression.** CD8+ T cells were in vitro stimulated and differentiated with CD3/CD28 antibodies under the Tc9-polarizing condition, with indicated treatments during the entire process. **(A)** Western blot analysis of Sumo1, -2, and -3 and LXRα/-β expression (left), and IP analysis of LXR and Sumo interaction and expression under indicated treatments (right) at day 4 after in vitro differentiation. **(B and C)** qRT-PCR (B) and ELISA (C) analyses of IL-9 expression or production, with or without 2-D08 treatment at day 4 after in vitro differentiation. **(D)** CD8+ T cells from *Lxra*−/− mice were in vitro stimulated and differentiated with CD3/CD28 antibodies under the Tc9-polarizing condition for 1 d and then transfected with LXRβ siRNA for 1 d, followed by the indicated treatments for additional 2 d. IL-9 production was measured under the indicated conditions. **(E)** Dual-luciferase analysis examined the impact of p50, p52, p65, RelB, and C-Rel overexpression on the *Il9* promoter in 293T cells. **(F)** Western blot analysis of p65 protein expression under β-CD or 2-D08 treatment at day 4 after in vitro differentiation. **(G)** P65 binding site prediction on the *Il9* promoter and ChIP analysis with p65 as baiting antibody under β-CD or 2-D08 treatment at day 4 after in vitro differentiation. **(H)** ChIP analysis of p65 binding under β-CD or 2-D08 treatment and indicated LXR deficiency conditions at day 4 after in vitro differentiation. Experiments were performed with at least three biological replicates and are representative of at least two independent experiments. Data are presented as mean ± SEM. *, P < 0.05; **. P < 0.01; ***, P < 0.001.

RORγ agonists, and cholesterol precursors are endogenous RORγ agonists that control Th17 differentiation (Hu et al., 2015), which provides evidence that cholesterol-related metabolites can regulate T cell differentiation.

IL-9 was initially considered as a Th2-specific cytokine (Stassen et al., 2012). Later, the discovery of IL-9–secreting Th9 (Dardalhon et al., 2008; Veldhoen et al., 2008) and Tc9 (Lu et al., 2014) cells brought a new life to the cytokine. In addition to CD4+ and CD8+ T cells, osteoblasts (Xiao et al., 2017), mucosal mast cells (Shik et al., 2017), and type 2 innate lymphoid cells (Rauber et

al., 2017) have also been reported to produce IL-9. However, the links between IL-9 and cancer progression are still elusive. IL-9 has been reported to promote the progression of many tumors in mice (Renauld et al., 1994) and humans (Fischer et al., 2003), whereas we and others showed that neutralizing IL-9 by injecting IL-9 antibodies to melanoma-bearing mice promoted tumor growth (Lu et al., 2012, 2014). Furthermore, our previous (Lu et al., 2014) and current study demonstrate a critical role of IL-9 in the antitumor function of Tc9 cells. Although IL-9–producing T cells have been identified in humans (Schlapbach et al., 2014),

and IL-9 was reported to promote the survival and function of human tumor-infiltrating T cells (Parrot et al., 2016), the role of IL-9 in antitumor response in human cancer remains elusive.

In our study, we used two generic products, simvastatin and lovastatin (Tobert, 2003), to reduce plasma cholesterol. According to the guidelines on cholesterol management (Grundy et al., 2004), simvastatin can be given to adults at 40 mg daily, which is comparable to the concentration (2 µM) used for CD8$^+$ T cell treatment in our study. In addition, IL-9 expression and production in human Tc9 cells can also be dramatically up-regulated by reducing cholesterol, demonstrating the translational potential to boost the antitumor function of Tc9 cells in human cancer.

Cholesterol homeostasis is tightly regulated by coordination of increasing and removing intracellular cholesterol (Spann and Glass, 2013). During these processes, many intermediates and derivatives are produced that participate in different signaling pathways. Oxysterols are generated during cholesterol metabolism through both enzymatic reactions and autoxidation. They regulate diverse cellular processes through transcription factors such as the LXRs and sterol regulatory element–binding proteins, and the G protein–coupled receptor EBI2. LXRs regulate cholesterol homeostasis by modulating expression of various genes, in particular, genes associated with cholesterol efflux (*Abca1* and *Abcg1*), thus eliminating excess cellular cholesterol (Spann and Glass, 2013; Traversari et al., 2014; Tall and Yvan-Charvet, 2015). It is unknown, however, whether LXR signaling can regulate IL-9 expression. The different effects of the oxysterols 22(R)-hydroxycholesterol and 22(S)-hydroxycholesterol on IL-9 production indicate a potential relationship between LXRs and *Il9* transcription, which led to our finding that *Il9* transcription was negatively regulated by the oxysterol–LXR–NF-κB axis. Although the oxysterols endogenously generated by cholesterol metabolism could also initiate cholesterol efflux processes (i.e., up-regulating *Abca1* gene expression; Zhang et al., 2013), our results showed that oxysterol-initiated feedback could not reverse cholesterol-induced IL-9 repression in Tc9 cells.

Although T cell transfer has been successful in the treatment of hematologic malignancies, great challenges remain in solid tumor immunotherapy. The limitation for tumor-infiltrating lymphocytes is the isolation and expansion with a conventional Tc1 condition. CAR-T cells are generated by engineering TCRs in T cells and have been shown to have powerful killing efficiency in hematologic malignancies (Shank et al., 2017). We have demonstrated that Tc9 cells exhibited an antitumor effect superior to that of traditional Tc1 cells in solid tumor models (Lu et al., 2014). To provide new strategies to improve the efficacy of CD8$^+$ T cells for clinical trials, the mechanism underlying this superior antitumor effect must be deciphered. One of the reasons for the superior antitumor effectiveness of Tc9 cells is their long-term functional persistence, which was not observed in Tc1 cells (Kalos and June, 2013; Perica et al., 2015; Baruch et al., 2017). Because the role of Th17 cells in cancers remains controversial, we did not include this population for comparison in our study. By reducing cholesterol during Tc9 cell differentiation in vitro, better Tc9 cells, with much longer persistence than normal Tc9 cells, were generated. These improved Tc9 cells retained the ability to convert to IFN-γ– and GzmB-expressing cells in vivo and

exerted a stronger antitumor effect compared with control Tc9 or Tc1 cells. Our study suggests that modulation of cholesterol may be an effective approach to improve the antitumor efficacy of adoptively transferred Tc9 cells, highlighting the importance of targeting lipid metabolism in cancer immunotherapy.

Materials and methods
Reagents and plasmids
Antibodies for flow cytometry were purchased from eBioscience. Antibodies for Western blot against Srebp1, Srebp2, LXRs, and Sumo1, -2, and -3 were purchased from Abcam, and other Western blot antibodies were purchased from Cell Signaling Technology. Cytokines were purchased from R&D Systems, and neutralization antibodies were purchased from Bio X Cell unless otherwise indicated. Cholesterol, 24(S)-hydroxycholesterol, 25-hydroxycholesterol, 7β-hydroxycholesterol, 20α-hydroxycholesterol, 3β-Hydroxy-5-cholesten-7-one, 22(R)-hydroxycholesterol, 22(S)-hydroxycholesterol, 5β-Cholestan-3β-ol, 5α-Cholest-7-en-3β-ol, 5,24-Cholestadien-3β-ol, 5-α-cholestane, β-cyclodextrin, simvastatin, lovastatin, and 2-D08 were purchased from Sigma-Aldrich. T0 and GW3965 were purchased from Cayman Chemical. Overexpression plasmids were purchased from Addgene unless otherwise indicated. All experiments were conducted according to the manufacturer's protocols unless otherwise indicated.

Mice
C57BL/6 mice were purchased from the National Cancer Institute. B6.Cg-Thy1a/Cy Tg(TcraTcrb)8Rest/J (Pmel-1), B6.129P2-Apoetm1Unc/J (*Apoe*$^{-/-}$), and B6.129S6-Nr1h3tm1Djm/J (*Lxra*$^{-/-}$) were purchased from the Jackson Laboratory. Pmel-1-*Il9*$^{-/-}$ mice and Pmel-1-*Il9r*$^{-/-}$ mice were produced by crossing Pmel-1 mice with *Il9*$^{-/-}$ mice or *Il9r*$^{-/-}$ mice. All experiments complied with protocols approved by the Institutional Animal Care and Use Committee at the Cleveland Clinic.

Cell purification and culture
T cells were isolated with EasySep Mouse CD8$^+$ T Cell Isolation kit or EasySep Mouse CD4$^+$ T Cell Isolation kit (STEMCELL Technologies, Inc.). Cells were stimulated and cultured with plate-bound anti-CD3 (2 µg/ml) and soluble anti-CD28 (1 µg/ml) antibodies in Th1/Tc1-, Th2/Tc2-, Th9/Tc9-, Th17/Tc17-, and T reg cell–polarizing conditions, respectively, with or without indicated treatments. After 3 d of differentiation, cells were transferred into a new well and cultured in normal T cell medium for another 2 d. In some experiments, splenocytes from Pmel-1 mice were directly stimulated with hgp100 peptide in Th1/Tc1-, Th2/Tc2-, Th9/Tc9-, Th17/Tc17-, and T reg cell–polarizing conditions, respectively. For the restimulation assay, after 5 d of differentiation, cells were counted and normalized to the counted cell number and then stimulated again with phorbol myristate acetate (50 ng/ml; Sigma-Aldrich) and ionomycin (500 ng/ml; Sigma-Aldrich) for indicated times.

Th1/Tc1-, Th2/Tc2-, Th9/Tc9-, Th17/Tc17-, and Treg polarizing–conditions
Cells were differentiated with plate-bound anti-CD3 (2 mg/ml) and soluble anti-CD28 (1 mg/ml) or hgp100$_{25-33}$ peptide (1 mg/ml;

Genscript) in the presence of indicated cytokines: Th1/Tc1 cells: IL-2 (10 ng/ml), IL-12 (10 ng/ml), and anti–IL-4 mAbs (5 µg/ml); Th2/Tc2 cells: IL-4 (10 ng/ml) and anti-IFNγ mAbs (10 µg/ml); Th9/Tc9 cells: IL-4 (10 ng/ml), TGF-β (1 ng/ml), and anti-IFNγ mAbs (10 µg/ml); Th17/Tc17 cells: IL-6 (30 ng/ml), TGF-β (2.5 ng/ml), anti–IL-4 mAbs (5 µg/ml), and anti-IFNγ mAbs (10 µg/ml); T reg cells: TGF-β (5 ng/ml) and IL-2 (10 ng/ml).

Human Tc9 cells
Peripheral blood mononuclear cells (PBMCs) from healthy donors were purchased from Gulf Coast Regional Blood Center. Informed consent was obtained for all subjects. PBMCs were isolated from buffy coat of healthy donors (Gulf Coast Regional Blood Center) by density gradient cell separation. Naive CD8^{+} T cells were isolated from PBMCs by negative selection kit (STEMCELL Technologies, Inc.) and stimulated with human T–activator CD3/CD28 Dynabeads (Invitrogen) with human IL-4 (10 ng/ml), human TGF-β1 (1 ng/ml), and anti-IFNγ (10 µg/ml) for 5 d. Cells were restimulated with PMA and ionomycin for 4 h with brefeldin A for intracellular IL-9 staining (phycoerythrin-anti–human IL-9; MH9A4; BioLegend). The study was approved by the Institutional Review Board at the Cleveland Clinic.

Gene microarray
Microarray analysis was performed using the Affymetrix WT Plus expression platform at the Gene Expression and Genotyping Facility at Case Western Reserve University.

qRT-PCR
Total RNA from T cells was extracted with TRIzol RNA isolation reagents (Invitrogen) or an RNeasy Mini kit (QIAGEN), followed by cDNA synthesis with the High-Capacity cDNA Reverse Transcription kit (Applied Biosystems). qRT-PCR was conducted with SYBR Select Master Mix (Applied Biosystems). Expression was normalized to the expression of the mouse housekeeping gene *Gapdh*.

Primers used are listed: *Hmgcr* forward: 5′-CACAATAACTTCCCAGGGGT-3′, *Hmgcr* reverse: 5′-GGCCTCCATTGAGATCCG-3′; *Sqle* forward: 5′-GATGGGCATTGAGACCTTCT-3′, *Sqle* reverse: 5′-TTTAAAAGAGCCCGACAGGA-3′; *Srebf2* forward: 5′-CTTTGATATACCAGAATGCAG-3′, *Srebf2* reverse: 5′-CAGGCTTTGGACTTGAGGCTG-3′; *Abca1* forward: 5′-GCTGCAGGAATCCAGAGAAT-3′, *Abca1* reverse: 5′-CATGCACAAGGTCCTGAGAA-3′; *Abcg1* forward: 5′-TTTCCCAGAGATCCCTTTCA-3′, *Abcg1* reverse: 5′-ATCGAATTCAAGGACCTTTCC-3′; *Idol* forward: 5′-CCTGCCAAGAGGGACTCTTTA-3′, *Idol* reverse: 5′-ACCGCCTTAAACTGAGGGTC-3′; *Ldlr* forward: 5′-CTAGCGATGCATTTTCCGTC-3′, *Ldlr* reverse: 5′-GTCATCGCCCTGCTCCTT-3′; *Il9* forward: 5′-AACAGTCCCTCCCTGTAGCA-3′, *Il9* reverse: 5′-AAGGATGATCCACCGTCAAA-3′; *Il4* forward: 5′-CGAGCTCACTCTCTGTGGTG-3′, *Il4* reverse: 5′-TGAACGAGGTCACAGGAGAA-3′; *Il10* forward: 5′-TGTCAAATTCATTCATGGCCT-3′, *Il10* reverse: 5′-ATCGATTTCTCCCCTGTGAA-3′; *Il21* forward: 5′-AAAACAGGCAAAAGCTGCAT-3′, *Il21* reverse: 5′-TGACATTGTTGAACAGCTGAAA-3′; *IFNγ* forward: 5′-TGAGCTCATTGAATGCTTGG-3′, *IFNγ* reverse: 5′-ACAGCAAGGCGAAAAGGAT-3′; *GzmB* forward: 5′-CATGTAGGGTCGAGAGTGGG-3′, *GzmB* reverse: 5′-CCTCCTGCTACTGCTGACCT-3′; *Irf4* forward:

5′-CAAAGCACAGAGTCACCTGG-3′, *Irf4* reverse: 5′-TGCAAGCTCTTTGACACACA-3′; *Pu.1* forward: 5′-TGCAGCTCTGTGAAGTGGTT-3′, *Pu.1* reverse: 5′-AGCGATGGAGAAAGCCATAG-3′; *Il9r* forward: 5′-AGCAGACCCAGCTGTAGATCA-3′, *Il9r* reverse: 5′-CCCTGGGAAGATGCATTG-3′.

Cholesterol content measurement
Cellular cholesterol content was measured using the Cholesterol Cell-Based Detection Assay kit (Cayman) and Amplex Red cholesterol assay kit (Invitrogen). For the cell-based detection assay, cells were stained with Filipin III and then examined using both confocal microscopy and flow cytometry. For cholesterol quantification, sterols were extracted with a sterol extraction kit (Sigma) and then analyzed using the Amplex Red cholesterol assay.

Flow cytometry
Cells were stimulated with phorbol myristate acetate and ionomycin and treated with brefeldin A (Biolegend) for 4 h before staining for intracellular cytokines with the BD Fixation/Permeabilization Solution kit. A CFSE dilution assay was performed using the CellTrace CFSE Cell Proliferation kit, according to the manufacturer's protocol. Cell surface markers were stained in flow cytometry staining buffer for 30 min on ice, washed twice, and results were then acquired using BD Calibur, BD Fortessa, or Miltenyi MACSQuant systems. Data were analyzed with FlowJo software (TreeStar).

Tumor models
Mice were injected subcutaneously in the abdomen with 5 × 10^{6} MC38-gp100 tumor cells. At 8 d after tumor injection, mice (five per group) were treated with adoptive transfer of 2 × 10^{6} indicated CD8^{+} T cells, followed by i.v. injection of 5 × 10^{5} peptide-pulsed, bone marrow–derived dendritic cells, generated as previously described (Lu et al., 2014). rhIL-2 was given at 6 × 10^{5} U i.p. daily for four doses after T cell transfer. As indicated, cyclophosphamide (Sigma-Aldrich) was administrated i.p. as a single dose at 250 mg/kg 1 d before T cell transfer. Mice were sacrificed at indicated days and analyzed. In some experiments, transferred T cells were sorted for indicated tissues. Tumor size was calculated as 0.5 × length × width[2].

In the B16 melanoma metastatic model, mice were injected i.v. with 10[5] B16 cells 2 d before adoptive transfer of 5 × 10^{5} indicated CD8^{+} T cells. At day 15 or 16 after tumor injection, mice were sacrificed and metastatic lung foci were counted.

T cell cytotoxicity
B16 target cells for Pmel-1 CD8^{+} T cells were labeled with 5 µM CFSE, whereas MC38 nontarget cells were labeled with 0.5 µM CFSE as the control. B16-target or MC38 nontarget control cells were incubated in duplicate with the Pmel-1 CD8^{+} T cells at different effector-to-target ratios. After 24 h, cells from each target and control well were mixed and analyzed by FACS. Percent specific lysis was calculated as (one target/control) × 100%.

Western blot and immunoprecipitation assays
Cell lysates and immunoblot were performed as previously described (Ma et al., 2015). Immunoprecipitation was conducted

Ma et al.
Cholesterol negatively regulates Tc9 cells

Journal of Experimental Medicine 1566
https://doi.org/10.1084/jem.20171576

according to the manufacturer's procedure (Abcam) and followed by Western blot analysis.

RNA interference of *Lxrb*
SiRNA targeting *Lxrb* was purchased from ThermoFisher and transfected into T cells with Lipofectamine RNAiMAX Transfection Reagent (ThermoFisher).

Viral transduction
Hmgcr and Abca1 shRNAs were synthesized and cloned into pLKO.1-GFP lentiviral vector. Viruses were packaged in 293T cells transfected with Lipofectamine 2000 (Life Science). Viral supernatant was harvested from day 1 to day 3, filtered with a 0.45-μm filter, concentrated with PEG-it Virus Precipitation Solution, and stored at –80°C till use. Tc9 cells were mixed with virus and 10 μg/ml protamine sulfate (Sigma) in a 24-well plate, followed by centrifugation at 1,800 rpm at 32°C for 2 h. After 2 h incubation, fresh culture medium was replaced. 3 d later, the cells and supernatant were harvested and followed by indicated experiments. ShRNA oligos: ShHmgcr 1 forward: 5′-CCGGGAACTTTGCAATCT AAGTTTACTCGAGTAAACTTAGATTGCAAAGTTCTTTTTG-3′, ShHmgcr 1 reverse: 5′-AATTCAAAAAGAACTTTGCAATCTAAG TTTACTCGAGTAAACTTAGATTGCAAAGTTC-3′; ShHmgcr 2 forward: 5′-CCGGGAGAATGTGATCGGATATATGCTCGAGCATATATC CGATCACATTCTCTTTTTG-3′, ShHmgcr 2 reverse: 5′-AATTCA AAAAGAGAATGTGATCGGATATATGCTCGAGCATATATCCGATCA CATTCTC-3′; ShAbca1 1 forward: 5′-CCGGCGCAGATATACCTAGCA TAACTCGAGTTATGCTAGGTATATCTAGCGTTTTTG-3′, ShAbca1 1 reverse: 5′-AATTCAAAAACGCTAGATATACCTAGCATAACTCGA GTTATGCTAGGTATATCTAGCG-3′; ShAbca1 2 forward: 5′-CCGGGA GTGCCACTTTCCGAATAAACTCGAGTTTATTCGGAAAGTGGCACT CTTTTTG-3′, ShAbca1 2 reverse: 5′-AATTCAAAAAGAGTGCCACTT TCCGAATAAACTCGAGTTTATTCGGAAAGTGGCACTC-3′.

Luciferase reporter assay
Mouse *Il9* promoter (from –895 to 5) was synthesized and subcloned into pGL4.10 vector (Promega). Luciferase was measured with the Dual-Luciferase Reporter Assay System according to the manufacturer's instructions (Promega).

ChIP assay
SimpleChIP Plus Enzymatic Chromatin IP kits were used for chromatin immunoprecipitation assays according to the manufacturer's protocol and measured by qRT-PCR. Chip primers: *Il9* promoter negative control, Forward: 5′-GCCTGCAAGTTTCTG GACAA-3′, reverse: 5′-GAATATGGGTGGGAGTGGGT-3′; NF-κB (approximately –65 to –55) forward: 5′-TCTGGAACTCAGTCTACC AGC-3′ NF-κB (approximately –65 to –55), reverse: 5′-TGGGCA CTGGGTATCAGTTTG-3′; NF-κB (approximately –448 to –438) forward: 5′-TTACAGGGGTGGTAATGAAGG-3′, NF-κB (approximately –448 to –438) reverse: 5′-GCAATCAAGTAAACTGAGGCT-3′.

CRISPR/Cas9 mediated IL-9–GFP reporter cell construction
CD8⁺ T cells were isolated from OT-I mice and stimulated under Tc9 or β-CD-Tc9 condition with plate-coated anti-CD3 and soluble anti-CD28 antibodies. On day 2, the cells were infected with IL-9 guide RNA lentivirus. On day 3, the cells were transfected with Cas9 and GFP template plasmids by electroporation kit (VPA-1006; Lonza). Cells were cultured for additional 2–3 d under Tc9 or β-CD-Tc9 condition for further experiments. The target sequence of *Il9* guide RNA is 5′-TACCAAATGCTAGCTAGC CC-3′ and was cloned into pCRISPR-LvSG03 plasmid. The Cas9 nuclease containing plasmid is CP-LvC9NU-01. DNA donor template plasmid for homology-directed repair of double-strand breaks is pDonor-D04 containing GFP cDNA with *Il9* homology sequences on both ends. All sequences and plasmids were commercially designed and constructed by Genecopoeia.

Data and materials availability
The microarray data accession numbers are GSE100422 and GSE111033.

Statistical analyses
For statistical analysis, Student's *t* test was used. A P value less than 0.05 was considered statistically significant. Results are presented as mean ± SEM unless otherwise indicated.

Online supplemental material
Fig. S1 depicts the impact of cholesterol modulation on IL-9 expression in CD8⁺ T cells. Fig. S2 depicts the impact of cholesterol modulation on CD8⁺ or CD4⁺ T cells. Fig. S3 depicts the knockdown efficiency and cholesterol concentration in Tc9, shRNA Hmgcr Tc9, and shRNA Abca1 Tc9 cells. Fig. S4 depicts the tumor models and cholesterol, IL-9 level, and T cell proliferation and apoptosis after adoptive transfer and experimental scheme of guide RNA, Cas9, and GFP template plasmid delivery to mouse CD8⁺ T cells for genome editing and phenotypic characterization by flow cytometry. Fig. S5 shows the effect of cholesterol modulation on TCR signaling, Th9/Tc9 transcription factor expression, and expression of LXRs and Sumo1, -2, and -3 in Tc9 cells.

Ma et al.
Cholesterol negatively regulates Tc9 cells

Journal of Experimental Medicine
https://doi.org/10.1084/jem.20171576

1567

References

Baruch, E.N., A.L. Berg, M.J. Besser, J. Schachter, and G. Markel. 2017. Adoptive T cell therapy: An overview of obstacles and opportunities. *Cancer.* 123(S11):2154–2162. https://doi.org/10.1002/cncr.30491

Bełtowski, J. 2008. Liver X receptors (LXR) as therapeutic targets in dyslipidemia. *Cardiovasc. Ther.* 26:297–316. https://doi.org/10.1111/j.1755-5922.2008.00062.x

Christian, A.E., M.P. Haynes, M.C. Phillips, and G.H. Rothblat. 1997. Use of cyclodextrins for manipulating cellular cholesterol content. *J. Lipid Res.* 38:2264–2272.

Dardalhon, V., A. Awasthi, H. Kwon, G. Galileos, W. Gao, R.A. Sobel, M. Mitsdoerffer, T.B. Strom, W. Elyaman, I.C. Ho, et al. 2008. IL-4 inhibits TGF-beta-induced Foxp3+ T cells and, together with TGF-beta, generates IL-9+ IL-10+ Foxp3(-) effector T cells. *Nat. Immunol.* 9:1347–1355. https://doi.org/10.1038/ni.1677

Fischer, M., M. Bijman, D. Molin, F. Cormont, C. Uyttenhove, J. van Snick, C. Sundström, G. Enblad, and G. Nilsson. 2003. Increased serum levels of interleukin-9 correlate to negative prognostic factors in Hodgkin's lymphoma. *Leukemia.* 17:2513–2516. https://doi.org/10.1038/sj.leu.2403123

Garcia-Hernandez, M.L., H. Hamada, J.B. Reome, S.K. Misra, M.P. Tighe, and R.W. Dutton. 2010. Adoptive transfer of tumor-specific Tc17 effector T cells controls the growth of B16 melanoma in mice. *J. Immunol.* 184:4215–4227. https://doi.org/10.4049/jimmunol.0902995

Gattinoni, L., C.A. Klebanoff, D.C. Palmer, C. Wrzesinski, K. Kerstann, Z. Yu, S.E. Finkelstein, M.R. Theoret, S.A. Rosenberg, and N.P. Restifo. 2005. Acquisition of full effector function in vitro paradoxically impairs the in vivo antitumor efficacy of adoptively transferred CD8+ T cells. *J. Clin. Invest.* 115:1616–1626. https://doi.org/10.1172/JCI24480

Gattinoni, L., X.S. Zhong, D.C. Palmer, Y. Ji, C.S. Hinrichs, Z. Yu, C. Wrzesinski, A. Boni, L. Cassard, L.M. Garvin, et al. 2009. Wnt signaling arrests effector T cell differentiation and generates CD8+ memory stem cells. *Nat. Med.* 15:808–813. https://doi.org/10.1038/nm.1982

Gattinoni, L., E. Lugli, Y. Ji, Z. Pos, C.M. Paulos, M.F. Quigley, J.R. Almeida, E. Gostick, Z. Yu, C. Carpenito, et al. 2011. A human memory T cell subset with stem cell-like properties. *Nat. Med.* 17:1290–1297. https://doi.org/10.1038/nm.2446

Grundy, S.M., J.I. Cleeman, C.N.B. Merz, H.B. Brewer Jr., L.T. Clark, D.B. Hunninghake, R.C. Pasternak, S.C. Smith Jr., N.J. Stone. National Heart, Lung, and Blood InstituteAmerican College of Cardiology Foundation. American Heart Association. 2004. Implications of recent clinical trials for the National Cholesterol Education Program Adult Treatment Panel III guidelines. *Circulation.* 110:227–239. https://doi.org/10.1161/01.CIR.0000133317.49796.0E

Hinrichs, C.S., R. Spolski, C.M. Paulos, L. Gattinoni, K.W. Kerstann, D.C. Palmer, C.A. Klebanoff, S.A. Rosenberg, W.J. Leonard, and N.P. Restifo. 2008. IL-2 and IL-21 confer opposing differentiation programs to CD8+ T cells for adoptive immunotherapy. *Blood.* 111:5326–5333. https://doi.org/10.1182/blood-2007-09-113050

Hinrichs, C.S., A. Kaiser, C.M. Paulos, L. Cassard, L. Sanchez-Perez, B. Heemskerk, C. Wrzesinski, Z.A. Borman, P. Muranski, and N.P. Restifo. 2009. Type 17 CD8+ T cells display enhanced antitumor immunity. *Blood.* 114:596–599. https://doi.org/10.1182/blood-2009-02-203935

Horton, J.D., J.L. Goldstein, and M.S. Brown. 2002. SREBPs: activators of the complete program of cholesterol and fatty acid synthesis in the liver. *J. Clin. Invest.* 109:1125–1131. https://doi.org/10.1172/JCI0215593

Hu, X., Y.H. Wang, L.Y. Hao, X.K. Liu, C.A. Lesch, B.M. Sanchez, J.M. Wendling, R.W. Morgan, T.D. Aicher, L.L. Carter, et al. 2015. Corrigendum: Sterol metabolism controls T(H)17 differentiation by generating endogenous ROR gamma agonists. *Nat. Chem. Biol.* 11:741. https://doi.org/10.1038/nchembio0915-741b

Ikonen, E. 2008. Cellular cholesterol trafficking and compartmentalization. *Nat. Rev. Mol. Cell Biol.* 9:125–138. https://doi.org/10.1038/nrm2336

Janssen, E.M., N.M. Droin, E.E. Lemmens, M.J. Pinkoski, S.J. Bensinger, B.D. Ehst, T.S. Griffith, D.R. Green, and S.P. Schoenberger. 2005. CD4+ T-cell help controls CD8+ T-cell memory via TRAIL-mediated activation-induced cell death. *Nature.* 434:88–93. https://doi.org/10.1038/nature03337

Joseph, S.B., A. Castrillo, B.A. Laffitte, D.J. Mangelsdorf, and P. Tontonoz. 2003. Reciprocal regulation of inflammation and lipid metabolism by liver X receptors. *Nat. Med.* 9:213–219. https://doi.org/10.1038/nm820

Kalos, M., and C.H. June. 2013. Adoptive T cell transfer for cancer immunotherapy in the era of synthetic biology. *Immunity.* 39:49–60. https://doi.org/10.1016/j.immuni.2013.07.002

Kaplan, M.H. 2013. Th9 cells: differentiation and disease. *Immunol. Rev.* 252:104–115. https://doi.org/10.1111/imr.12028

Klebanoff, C.A., S.E. Finkelstein, D.R. Surman, M.K. Lichtman, L. Gattinoni, M.R. Theoret, N. Grewal, P.J. Spiess, P.A. Antony, D.C. Palmer, et al. 2004. IL-15 enhances the in vivo antitumor activity of tumor-reactive CD8+ T cells. *Proc. Natl. Acad. Sci. USA.* 101:1969–1974. https://doi.org/10.1073/pnas.0307298101

Klebanoff, C.A., L. Gattinoni, P. Torabi-Parizi, K. Kerstann, A.R. Cardones, S.E. Finkelstein, D.C. Palmer, P.A. Antony, S.T. Hwang, S.A. Rosenberg, et al. 2005. Central memory self/tumor-reactive CD8+ T cells confer superior antitumor immunity compared with effector memory T cells. *Proc. Natl. Acad. Sci. USA.* 102:9571–9576. https://doi.org/10.1073/pnas.0503726102

Lu, Y., S. Hong, H. Li, J. Park, B. Hong, L. Wang, Y. Zheng, Z. Liu, J. Xu, J. He, et al. 2012. Th9 cells promote antitumor immune responses in vivo. *J. Clin. Invest.* 122:4160–4171. https://doi.org/10.1172/JCI65459

Lu, Y., B. Hong, H. Li, Y. Zheng, M. Zhang, S. Wang, J. Qian, and Q. Yi. 2014. Tumor-specific IL-9-producing CD8+ Tc9 cells are superior effector than type-I cytotoxic Tc1 cells for adoptive immunotherapy of cancers. *Proc. Natl. Acad. Sci. USA.* 111:2265–2270. https://doi.org/10.1073/pnas.1317431111

Ma, X., Q. Wang, Y. Liu, Y. Chen, L. Zhang, M. Jiang, X. Li, R. Xiang, R.Q. Miao, Y. Duan, and J. Han. 2015. Inhibition of tumor growth by U0126 is associated with induction of interferon-γ production. *Int. J. Cancer.* 136:771–783. https://doi.org/10.1002/ijc.29038

Maxwell, K.N., R.E. Soccio, E.M. Duncan, E. Sehayek, and J.L. Breslow. 2003. Novel putative SREBP and LXR target genes identified by microarray analysis in liver of cholesterol-fed mice. *J. Lipid Res.* 44:2109–2119. https://doi.org/10.1194/jlr.M300203-JLR200

Mittrücker, H.W., A. Visekruna, and M. Huber. 2014. Heterogeneity in the differentiation and function of CD8+ T cells. *Arch. Immunol. Ther. Exp. (Warsz.).* 62:449–458. https://doi.org/10.1007/s00005-014-0293-y

Miyagawa, F., H. Zhang, A. Terunuma, K. Ozato, Y. Tagaya, and S.I. Katz. 2012. Interferon regulatory factor 8 integrates T-cell receptor and cytokine-signaling pathways and drives effector differentiation of CD8 T cells. *Proc. Natl. Acad. Sci. USA.* 109:12123–12128. https://doi.org/10.1073/pnas.1201453109

Parrot, T., M. Allard, R. Oger, H. Benlalam, D. Raingeard de la Blétière, A. Coutolleau, L. Preisser, J. Desfrançois, A. Khammari, B. Dréno, et al. 2016. IL-9 promotes the survival and function of human melanoma-infiltrating CD4(+) CD8(+) double-positive T cells. *Eur. J. Immunol.* 46:1770–1782. https://doi.org/10.1002/eji.201546061

Perica, K., J.C. Varela, M. Oelke, and J. Schneck. 2015. Adoptive T cell immunotherapy for cancer. *Rambam Maimonides Med. J.* 6:e0004. https://doi.org/10.5041/RMMJ.10179

Rauber, S., M. Luber, S. Weber, L. Maul, A. Soare, T. Wohlfahrt, N.Y. Lin, K. Dietel, A. Bozec, M. Herrmann, et al. 2017. Resolution of inflammation by interleukin-9-producing type 2 innate lymphoid cells. *Nat. Med.* 23:938–944.

Renauld, J.C., N. van der Lugt, A. Vink, M. van Roon, C. Godfraind, G. Warnier, H. Merz, A. Feller, A. Berns, and J. Van Snick. 1994. Thymic lymphomas in interleukin 9 transgenic mice. *Oncogene.* 9:1327–1332.

Restifo, N.P., M.E. Dudley, and S.A. Rosenberg. 2012. Adoptive immunotherapy for cancer: harnessing the T cell response. *Nat. Rev. Immunol.* 12:269–281. https://doi.org/10.1038/nri3191

Rosenberg, S.A., N.P. Restifo, J.C. Yang, R.A. Morgan, and M.E. Dudley. 2008. Adoptive cell transfer: a clinical path to effective cancer immunotherapy. *Nat. Rev. Cancer.* 8:299–308. https://doi.org/10.1038/nrc2355

Schlapbach, C., A. Gehad, C. Yang, R. Watanabe, E. Guenova, J.E. Teague, L. Campbell, N. Yawalkar, T.S. Kupper, and R.A. Clark. 2014. Human T$_H$9 cells are skin-tropic and have autocrine and paracrine proinflammatory capacity. *Sci. Transl. Med.* 6:219ra8. https://doi.org/10.1126/scitranslmed.3007828

Shank, B.R., B. Do, A. Sevin, S.E. Chen, S.S. Neelapu, and S.B. Horowitz. 2017. Chimeric Antigen Receptor T Cells in Hematologic Malignancies. *Pharmacotherapy.* 37:334–345. https://doi.org/10.1002/phar.1900

Sharpe, L.J., E.C. Cook, N. Zelcer, and A.J. Brown. 2014. The UPS and downs of cholesterol homeostasis. *Trends Biochem. Sci.* 39:527–535. https://doi.org/10.1016/j.tibs.2014.08.008

Shik, D., S. Tomar, J.B. Lee, C.Y. Chen, A. Smith, and Y.H. Wang. 2017. IL-9-producing cells in the development of IgE-mediated food allergy. *Semin. Immunopathol.* 39:69–77. https://doi.org/10.1007/s00281-016-0605-x

Spann, N.J., and C.K. Glass. 2013. Sterols and oxysterols in immune cell function. *Nat. Immunol.* 14:893–900. https://doi.org/10.1038/ni.2681

Stassen, M., E. Schmitt, and T. Bopp. 2012. From interleukin-9 to T helper 9 cells. *Ann. N. Y. Acad. Sci.* 1247:56–68. https://doi.org/10.1111/j.1749-6632.2011.06351.x

Swamy, M., K. Beck-Garcia, E. Beck-Garcia, F.A. Hartl, A. Morath, O.S. Yousefi, E.P. Dopfer, E. Molnár, A.K. Schulze, R. Blanco, et al. 2016. A Cholesterol-Based Allostery Model of T Cell Receptor Phosphorylation. *Immunity.* 44:1091–1101. https://doi.org/10.1016/j.immuni.2016.04.011

Tall, A.R., and L. Yvan-Charvet. 2015. Cholesterol, inflammation and innate immunity. *Nat. Rev. Immunol.* 15:104–116. https://doi.org/10.1038/nri3793

Tobert, J.A. 2003. Lovastatin and beyond: the history of the HMG-CoA reductase inhibitors. *Nat. Rev. Drug Discov.* 2:517–526. https://doi.org/10.1038/nrd1112

Topalian, S.L., C.G. Drake, and D.M. Pardoll. 2015. Immune checkpoint blockade: a common denominator approach to cancer therapy. *Cancer Cell.* 27:450–461. https://doi.org/10.1016/j.ccell.2015.03.001

Traversari, C., S. Sozzani, K.R. Steffensen, and V. Russo. 2014. LXR-dependent and -independent effects of oxysterols on immunity and tumor growth. *Eur. J. Immunol.* 44:1896–1903. https://doi.org/10.1002/eji.201344292

Twyman-Saint Victor, C., A.J. Rech, A. Maity, R. Rengan, K.E. Pauken, E. Stelekati, J.L. Benci, B. Xu, H. Dada, P.M. Odorizzi, et al. 2015. Radiation and dual checkpoint blockade activate non-redundant immune mechanisms in cancer. *Nature.* 520:373–377. https://doi.org/10.1038/nature14292

Veldhoen, M., C. Uyttenhove, J. van Snick, H. Helmby, A. Westendorf, J. Buer, B. Martin, C. Wilhelm, and B. Stockinger. 2008. Transforming growth factor-beta 'reprograms' the differentiation of T helper 2 cells and promotes an interleukin 9-producing subset. *Nat. Immunol.* 9:1341–1346. https://doi.org/10.1038/ni.1659

Visekruna, A., J. Ritter, T. Scholz, L. Campos, A. Guralnik, L. Poncette, H. Raifer, S. Hagner, H. Garn, V. Staudt, et al. 2013. Tc9 cells, a new subset of CD8(+) T cells, support Th2-mediated airway inflammation. *Eur. J. Immunol.* 43:606–618. https://doi.org/10.1002/eji.201242825

Wang, F., K. Beck-García, C. Zorzin, W.W. Schamel, and M.M. Davis. 2016. Inhibition of T cell receptor signaling by cholesterol sulfate, a naturally occurring derivative of membrane cholesterol. *Nat. Immunol.* 17:844–850. https://doi.org/10.1038/ni.3462

Xiao, M., Y. Wang, C. Tao, Z. Wang, J. Yang, Z. Chen, Z. Zou, M. Li, A. Liu, C. Jia, et al. 2017. Osteoblasts support megakaryopoiesis through production of interleukin-9. *Blood.* 129:3196–3209. https://doi.org/10.1182/blood-2016-11-749838

Xiao, X., S. Balasubramanian, W. Liu, X. Chu, H. Wang, E.J. Taparowsky, Y.X. Fu, Y. Choi, M.C. Walsh, and X.C. Li. 2012. OX40 signaling favors the induction of T(H)9 cells and airway inflammation. *Nat. Immunol.* 13:981–990. https://doi.org/10.1038/ni.2390

Yang, W., Y. Bai, Y. Xiong, J. Zhang, S. Chen, X. Zheng, X. Meng, L. Li, J. Wang, C. Xu, et al. 2016. Potentiating the antitumour response of CD8(+) T cells by modulating cholesterol metabolism. *Nature.* 531:651–655. https://doi.org/10.1038/nature17412

Zhang, L., M. Jiang, Y. Shui, Y. Chen, Q. Wang, W. Hu, X. Ma, X. Li, X. Liu, X. Cao, et al. 2013. DNA topoisomerase II inhibitors induce macrophage ABCA1 expression and cholesterol efflux-an LXR-dependent mechanism. *Biochim. Biophys. Acta.* 1831:1134–1145. https://doi.org/10.1016/j.bbalip.2013.02.007

Zhang, T., P. Dai, D. Cheng, L. Zhang, Z. Chen, X. Meng, F. Zhang, X. Han, J. Liu, J. Pan, et al. 2014a. Obesity occurring in apolipoprotein E-knockout mice has mild effects on fertility. *Reproduction.* 147:141–151. https://doi.org/10.1530/REP-13-0470

Zhang, Y., F. Hou, X. Liu, D. Ma, Y. Zhang, B. Kong, and B. Cui. 2014b. Tc17 cells in patients with uterine cervical cancer. *PLoS One.* 9:e86812. https://doi.org/10.1371/journal.pone.0086812